Available online at www.sciencedirect.com
ScienceDirect
Polymer 48 (2007) 5398–5407
polymer
www.elsevier.com/locate/polymer

Melting behavior of poly(L-lactic acid): Effects of crystallization temperature and time

Munehisa Yasuniwa*, Koji Iura, Yusuke Dan

Department of Applied Physics, Faculty of Science, Fukuoka University, 8-19-1 Nanakuma, Jonan-ku, Fukuoka 814-0180, Japan

Received 17 May 2007; received in revised form 5 July 2007; accepted 8 July 2007
Available online 14 July 2007

Abstract

Effects of crystallization temperature and time on the melting behavior of poly(L-lactic acid) were studied with differential scanning calorimetry (DSC). The isothermal crystallization was performed at various temperatures (T_cs), and DSC melting curves for the isothermally crystallized samples were obtained at 10 K min^{-1}. When T_c was lower than T_d ($\sim$135 °C), the double melting peaks appeared. The melting behavior, especially T_c dependence of the melting temperature (T_m), discretely changed at T_b (=113 °C), in accordance with the discrete change of the crystallization behavior at T_b, which was previously reported. When T_c was higher than T_d, a single melting peak appeared. In addition, T_c dependence of dT_m/dT_c discretely changed at T_d. That is, the melting behavior, especially T_c dependence of T_m and dT_m/dT_c, are different in three temperature regions of T_c divided by T_b and T_d: Regions I ($T_c \leq T_b$), II ($T_b \leq T_c \leq T_d$), and III ($T_d \leq T_c$). The effect of crystallization time on the melting behavior, melting temperature and heat of fusion in each temperature region of T_c is also discussed.

Keywords: Poly(L-lactic acid) (PLLA); Differential scanning calorimetry (DSC); Melting behavior

1. Introduction

Poly(L-lactic acid) (PLLA), an environmentally degradable polymer, has an ideal combination of attractive properties, such as high melting points, good mechanical properties, barrier to flavor and aroma. Accordingly, PLLA is currently investigated for a large number of commodity applications [1,2], and its melting and crystallization behaviors have been characterized with various experimental techniques [3]. However, the melting behavior of PLLA has been reported by a small number of researchers [4–23].

In 2006, Yasuniwa and coworkers elucidated the discrete change of the crystallization behavior of PLLA: T_c dependence of peak crystallization time (τ_p) and linear growth rate of spherulite (G) of the isothermally crystallized sample discretely change at 113 °C (=T_b) [24]. In addition, they found that the crystal structure of the isothermally crystallized sample also discretely changes at T_b. The crystal structure for $T_c < T_b$ was obviously different from that for $T_b < T_c$. They suggested that the origin of the discrete change in the T_c dependence of τ_p and G is attributed to the discrete change of the crystal structure. Since the melting behavior of a semicrystalline polymer largely depends on the preceding crystallization process, it is reasonable to deduce that T_c dependence of the melting behavior of an isothermally crystallized PLLA sample also discretely changes at T_b. However, the discrete change in the melting behavior of PLLA has not yet been reported except for our preliminary report of this article [18].

Yasuniwa and coworkers [17] studied the melting process of non-isothermally melt-crystallized PLLA samples by differential scanning calorimetry (DSC) and reported the double melting behavior of PLLA. They illustrated the appearance region of the double melting in a cooling rate–heating rate map (CR–HR map). Then the double melting behavior of

* Corresponding author.
E-mail address: yasuniwa@fukuoka-u.ac.jp (M. Yasuniwa).

0032-3861/$ - see front matter © 2007 Elsevier Ltd. All rights reserved.
doi:10.1016/j.polymer.2007.07.012

an isothermally melt-crystallized PLLA sample was studied by several authors [18–20,22,23], and they reported crystallization temperature dependence of the melting temperature and crystallinity with no discrete change [19,20].

The double melting behavior has been reported for many semicrystalline polymers: poly(ethylene terephthalate) [25–27], poly(butylene terephthalate) (PBT) [28–30], poly(butylene naphthalate) (PBN) [31–33], poly(ether ether ketone) [34–36], poly(butylene succinate) (PBSu) [37–39], and so on. Many authors have explained the origin of the double melting behavior by the melt-recrystallization model: The melting of semicrystalline polymers proceeds through the melting of original crystals, recrystallization, and the melting of recrystallized crystals. The recrystallization in the melting process was proved for PBT and PBN by an increase of crystallinity with X-ray analysis [29,32,33]. The double melting behavior of PLLA has also been explained by the melt-recrystallization mechanism [17–23], although solid proof of the recrystallization in PLLA has not been presented.

An isothermally crystallized sample (ICS), which is prepared by the crystallization at a constant temperature (T_c) after rapid cooling from the melt, and a non-isothermally crystallized sample (NCS), which is prepared by the cooling at a constant cooling rate (CR) from the melt, are usually used for the analysis of the melting behavior. Because the crystallization for the NCS occurs in a certain temperature range, a distribution of the thermal stability of the crystallites in the ICS is narrower than that in the NCS. Therefore, the effect of crystallization condition on the melting behavior should be accurately analyzed by the use of the ICS.

The purpose of this series of articles is to clarify the multiple melting behavior of PLLA and the origin of the complex melting behavior. Especially, it is an important purpose to elucidate how the discrete change in the preceding crystallization process affects the melting behavior. We performed thermal and X-ray analyses to clarify fundamental aspects of the melting process using the ICS. As the first step of this investigation, the melting behavior of the ICSs, particularly the effect of the crystallization condition, crystallization temperature and crystallization time, on the multiple melting behavior, is studied in this article.

2. Experimental

2.1. Sample preparation

An additive free PLLA experimental resin in a pellet form was purchased from General Science Co. Molecular weight of the sample was measured with a gel permeation chromatography (GPC) by Taki Chemical Co., Ltd. Number-averaged molecular weight (M_n) and weight-averaged molecular weight (M_w) of the former sample were 4.8×10^4 and 9.1×10^4, respectively. These values were calibrated by polystyrene standards. Optical rotatory power, $[\alpha]_D^{25}$, of the sample, which was also measured by them at a wavelength of 589 nm using 0.1% chloroform solution at 25 °C, was −156. The pellets were heated and kept in a vacuum oven at 120 °C for 24 h for the removal of any residual moisture before they were measured.

2.2. Apparatus

A thermal analysis was carried out with a differential scanning calorimeter (Perkin–Elmer Pyris 1). The temperature of the DSC apparatus was calibrated with biphenyl, indium, and zinc. The heat of fusion was also calibrated with indium. A PLLA sample of 5.0 ± 0.1 mg was sealed in an aluminum sample pan for DSC. Samples were used for DSC and were always kept under a dry nitrogen atmosphere.

Wide-angle X-ray diffraction (WAXD) patterns were obtained at room temperature (ca. 20 °C) with a WAXD measurement system reported elsewhere [29]. Monochromatized Cu Kα radiation (=1.542 Å) was used as an incident X-ray beam. The diffracted X-ray intensity was detected with a position-sensitive proportional counter (PSPC) system. The diffraction angles reported for α-aluminum oxide (α-Al_2O_3) were used as standard: The angles of the diffraction patterns were corrected with three diffraction angles of α-Al_2O_3 for the Cu Kα radiation: 25.296°, 35.152°, and 37.801°, corresponding to the reflection lines of (012), (104), and (110), respectively [40].

2.3. Heating and cooling conditions

Vasanthakumari and Pennings [41] and Tsuji and Ikada [42] reported equilibrium melting temperatures T_m^os for PLLA as 207 and 205 °C, respectively. In our experiment, samples were held in a molten state (210 °C) for 10 min to remove any crystal nuclei in the samples. The melted samples were cooled to a predetermined crystallization temperature (T_c) at a rate of 70 K min^{-1}, and the isothermal crystallization was performed at various T_cs ranging from 80 to 140 °C during various crystallization times. The crystallization times were determined from T_c dependence of the peak crystallization time (Fig. 2) reported in the previous article: The ICS was prepared at the crystallization time of approximately four times of the peak crystallization time (τ_p) at each T_c. After the isothermal crystallization, the sample was rapidly cooled to 30 °C at a rate of 70 K min^{-1} to prevent additional crystallization during cooling from T_c and held for 10 min at 30 °C. DSC curves for the ICSs were obtained at a heating rate (HR) of 10 K min^{-1}. Because melting and recrystallization occurs competitively during heating, melting process largely depends on a starting temperature of the heating. Starting temperature of all DSC measurements was fixed to 30 °C which is lower than the glass transition temperature. Heat of fusion was obtained from DSC curves by the following procedure. After the subtraction of a contribution of the heat capacity of a sample pan, the baseline of the DSC curve was drawn between 100 and 200 °C. Then, the total contribution of the endothermic (positive) and exothermic (negative) peaks in the DSC curve was calculated.

3. Results

3.1. Discrete change of the melting behavior and double melting

Fig. 1a and b shows the DSC curves of ICSs obtained at the indicated T_cs. Crystallization times are indicated in the figure. Double endothermic peaks, low- and high-temperature peaks denoted by L (LI, LII, LIII) and H, evidently appear in the DSC curves of the ICSs. The reason for the notation of LI, LII, and LIII will be shown in the next paragraph. Furthermore, an exothermic peak between L and H is assigned as R. The appearance of L, R and H originates from the melting of original crystals, recrystallization, and the melting of recrystallized crystals, respectively. Outline of the mechanism for the appearance of these peaks has been explained elsewhere [17,29,32,38,39]. The scale of the heat flow rate of the every DSC curve is normalized so that peak heights of the DSC curves can be compared with one another. For ease of comparison between DSC peaks shown in Fig. 1a and b, the same DSC curve for the ICS(115 °C) is shown in Fig. 1a and b.

As can be seen in the figure, T_c dependence of the peak profiles of the DSC curves discretely changes at T_b (=113 °C): peak L (LII) predominantly appears in the high-temperature region ($T_b < T_c$), whereas peak H predominantly appears in the low temperature region ($T_c < T_b$). In addition, T_c dependence on the peak profiles changes at T_d (~135 °C): L (LIII) appears as a single peak in the temperature region $T_d < T_c$, whereas L (LII) appears with H as double peaks in the temperature region $T_b < T_c < T_d$. Consequently, T_c can be divided in three temperature regions, Regions I ($T_c \leq T_b$), II ($T_b \leq T_c \leq T_d$), and III ($T_d \leq T_c$). Peaks L in Regions I, II, and III are denoted by LI, LII, and LIII, respectively.

As shown in our previous article [24], discrete change of the crystallization behavior occurs at T_b (=113 °C). In accordance with the crystallization behavior, melting behavior also changes at T_b as shown in the figure. That is, the value of 113 °C for the discrete change of the melting behavior shown in the figure originates from the discrete change of the crystallization behavior. In contrast, the value of T_d cannot be accurately determined, because disappearance of H is not discernible in the DSC peak in which H is incorporated in L. Besides, peak profiles change with crystallization time of the ICS. Therefore, it is better to consider that melting behavior changes around 135 °C, that is, T_d.

The peak melting temperatures of L (LI, LII, LIII) and H were obtained from the DSC curves and are expressed by T_m(L) and T_m(H), respectively. T_c dependence of these temperatures is shown in Fig. 2. The solid and dashed lines in the figure show the fitting curves of these temperatures. The characteristic temperatures, T_b and T_d, are shown by dash–dotted lines.

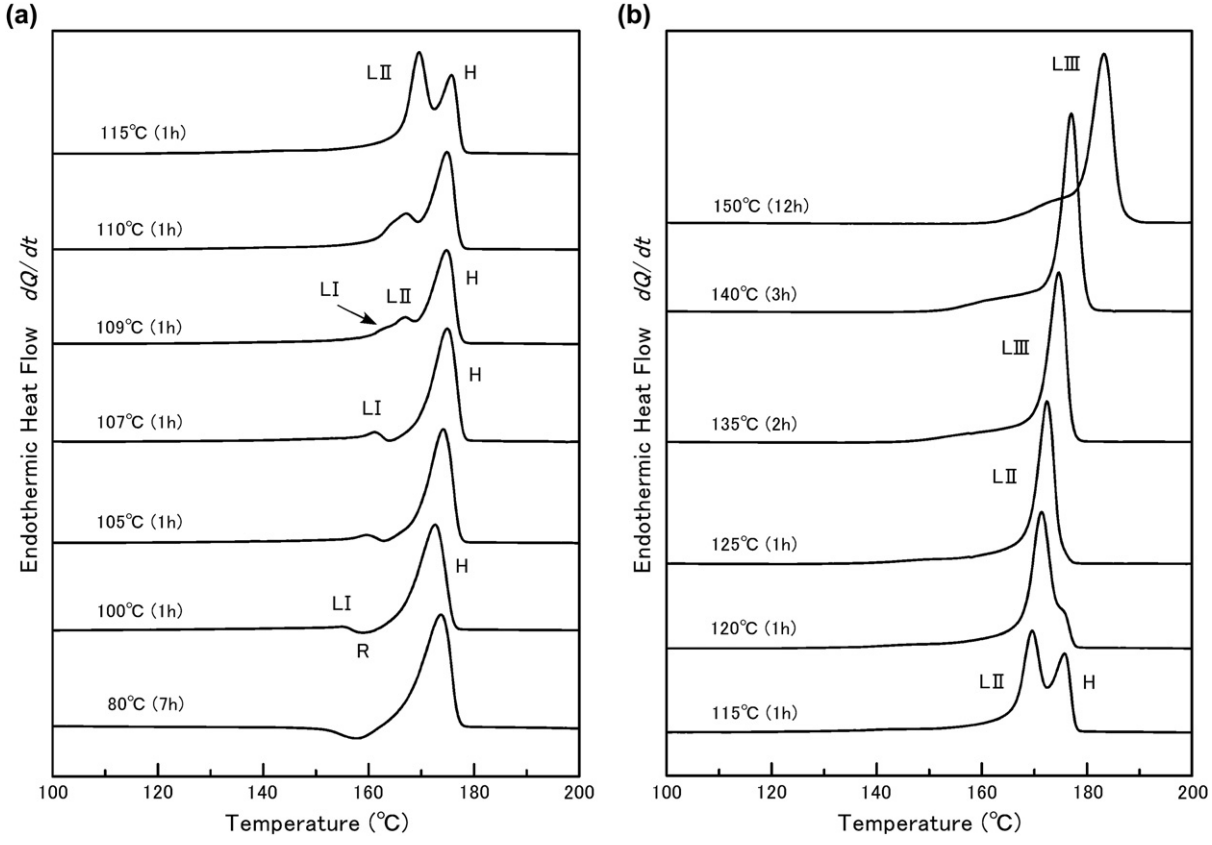

Fig. 1. DSC curves of the ICSs obtained at the indicated T_cs and crystallization times: (a) for ICS($T_c \leq 115$ °C) and (b) for ICS($T_c \geq 115$ °C). The HR of the DSC scans was 10 K min^{-1}.

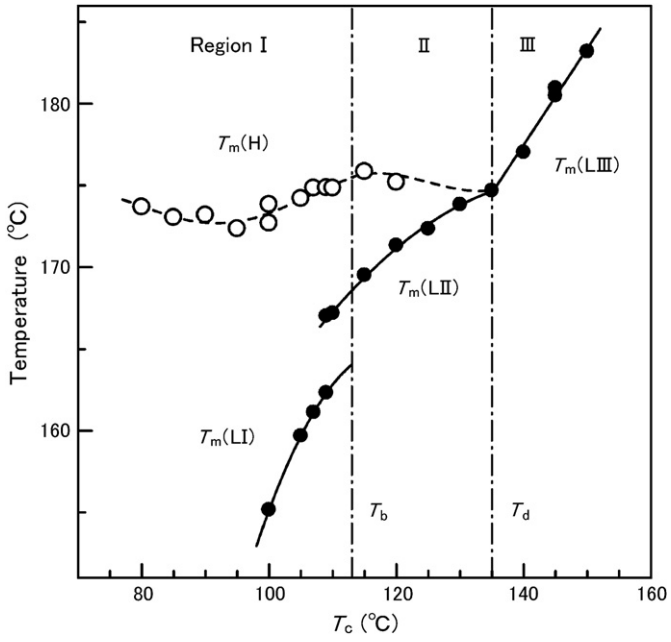

Fig. 2. T_c dependence of (●) T_m(L) and (○)T_m(H) obtained from the DSC curves. The HR of the DSC scans was 10 K min^{-1}. The solid and broken lines show the fitting curves of these temperatures. The dash-dotted lines show T_b and T_d.

T_c dependence of T_m(L) discretely changes at T_b in accordance with the change of the crystallization behavior: T_m(LI) discontinuously increases to T_m(LII) by 4.5 K at T_b. Besides, profiles of the fitting curves in Regions I and II are completely different with each other. Since T_m(L) corresponds to the melting temperature of the crystals in the ICS, the change in the T_c dependence of T_m(L) and the difference of fitting curve profiles can be interpreted by the difference of the crystal structures in Regions I and II [24]. In contrast, T_m(L) almost continuously changes around T_d at which there is no change of the crystal structure, but T_c dependence of T_m(L), $dT_m(L)/dT_c$, discretely changes between Regions II and III. The value of 135 °C for T_d was determined from the temperature of an intersection of fitting curves for T_m(LII) and T_m(LIII). There is enough possibility that this value changes with crystallization conditions from the melt and heating conditions of an ICS. Therefore, T_d could not be definitely concluded and is expressed as around 135 °C or T_d (~135 °C).

In our previous article [24], the crystal structures of the ICSs for $T_c < T_b$ (Region I) and $T_b < T_c$ (Regions II and III) were assigned to trigonal one (β-form) [43] and orthorhombic one (α-form) [44–46], respectively. However, crystal structure for $T_c < T_b$ could not be definitely determined from the X-ray diffraction pattern because of a small number of diffraction peaks as mentioned in Ref. [24]. On the other hand, the investigation on the crystal structure for $T_c < T_b$ is now in progress. Recently, Zhang and coworkers suggested α′-form (pseudo-orthorhombic) which is assigned to the disordered phase of the α-form [47,48]. It seems that there is no general consensus about crystal structure in Region I [43,47–49]. Taking account of these circumstances, hereafter LTC and HTC are used for the names of crystals of the low- and high- temperature modifications.

We performed wide-angle X-ray analysis on the heating process of ICSs and confirmed the transition from the LTC to the orthorhombic crystal before final melting in Region I. In contrast, crystal structure did not change up to final melting in Regions II and III. That is, H corresponds to the melting of the orthorhombic crystal over the whole temperature region, and L corresponds to that of the LTC in Region I and the orthorhombic crystal in Regions II and III. T_c dependence of melting temperatures is complex in comparing with other semicrystalline polymers as shown in Fig. 2. The complexity originates from the combination of the double melting behavior and crystal polymorphism.

Fig. 3 shows the T_c dependence of heat of fusion ΔQ obtained from the DSC curves. T_c dependence of ΔQ was fitted by linear equations in every temperature region, Region I, II, or III. The characteristic temperatures, T_b and T_d, are shown by dash–dotted lines in the figure.

As shown in Fig. 3, the slope of the fitting curve in Region I is smaller than those of the other regions. Although there are discontinuous changes of the melting behavior at T_b and T_d, roughly speaking, the value of ΔQ of the ICSs monotonously increase from about 51.0 to 77.5 J g^{-1} with T_c. Because the heat of fusion ΔQ is proportional to the crystallinity of the ICSs, the crystallinity also increases with T_c. That is, Fig. 3 also shows the T_c dependence of the crystallinity. Fisher and coworkers [50] and Pyda and coworkers [51] reported the heat of fusion for a perfect crystal of PLLA to be 93 J g^{-1} and 91 J g^{-1}, respectively. The crystallinity of the ICSs can be estimated from these values. It changes from about 55 to 85% with T_c.

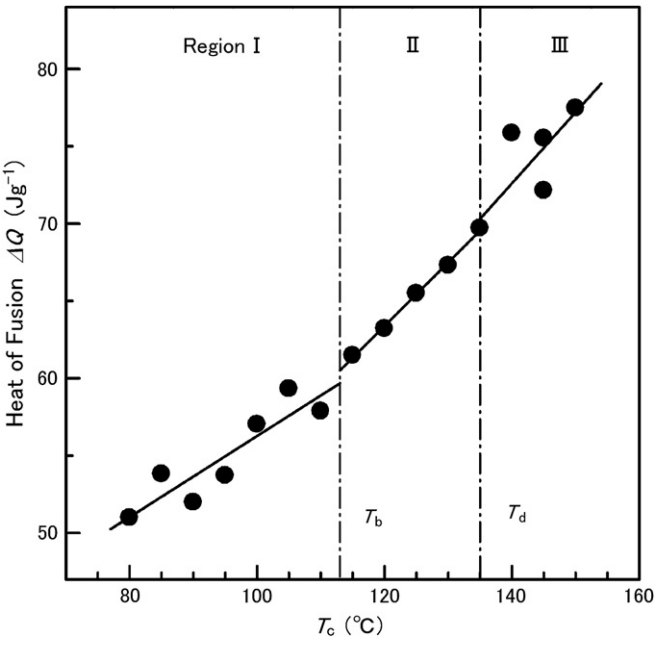

Fig. 3. T_c dependence of ΔQ calculated from the DSC curves. The solid lines show the fitting curves of ΔQ values. The dash-dotted lines show T_b and T_d.

Since the melting and recrystallization occur competitively in the heating process, the endothermic heat flow due to melting and the exothermic heat flow due to recrystallization cancel out each other. As shown in Fig. 1, the DSC curve shows straight line in the temperature range lower than 140 °C in spite of the progress of the melting. The melt-recrystallization occurs from a low temperature in Region I because of the low thermal stability of the crystals in the ICS. Consequently, the base lines for the DSC curves for the ICSs(Region I) shown in Fig. 1 could not be accurately determined. Therefore, it is considered that ΔQ was underestimated by the deflection of the baseline in Region I. In addition, as shown in Fig. 3, deviation of each datum from the fitting curve in Region I is large in comparison with Region II. The deviation may originate from the determination of the baseline.

The characteristics of the melting behavior in three temperature regions, which were obtained from the present investigation shown in Figs. 1–3, are as follows.

Region I ($T_c \leq T_b$): Peaks H and R appear in the DSC curve of the ICS(80 °C), whereas LI does not appear. The disappearance of LI is due to the melt-recrystallization and it originates from the low thermal stability of the crystals in the sample. The thermal stability of the ICS increases with T_c. As a result, LI increases with T_c as shown in the DSC curves of the ICSs(100–110 °C), whereas R decreases. In addition, T_m(LI) abruptly increases by the increase of T_c. This result indicates the abrupt increase of crystals' sizes in the ICSs(100–110 °C) with T_c. DSC curve of the ICS(110 °C) shows three endothermic peaks, LI, LII, and H. It corresponds to an intermediate one of Regions I and II.

Peak H corresponds to the melting of the recrystallized crystals. Although L and R changes with T_c, H does not change as shown in Fig. 1. This result indicates that the formation of the recrystallized crystal through the heating process is almost constant, although the crystallinity of the starting sample of DSC, that is, the ICS, changes with T_c as shown in Fig. 3. In contrast, T_m(H) slightly increases with T_c at $T_c \geq 100$ °C as shown in Fig. 2, whereas it is almost constant at $T_c \leq 100$ °C. The temperature range where the slight increase of T_m(H) is observed corresponds to the temperature range where the increase of T_m(LI) is observed. Since the increase of T_m(H) indicates the increase of the crystal size in the heating process, it can be deduced that the increase of the crystal size of the starting sample (ICS) results in the increase of the crystal size of the recrystallized crystals. That is, the thermal stability of the recrystallized crystal is increased by the increase of the thermal stability of the ICS in this region.

Region II ($T_b \leq T_c \leq T_d$): The typical double melting behavior is observed in this region. Peak LII increases with increasing T_c as shown in Fig. 1, whereas H decreases. On the other hand, T_m(LII) increases with increasing T_c, whereas T_m(H) is almost constant. Peak H does not appear evidently in the DSC curves of the ICS(125, 130 °C), however, the peak width of LII is slightly broad. The broad endothermic peak indicates the overlapping of H on LII.

When the peak of LII overlaps on that of H, T_m(H) determined from the DSC peak decreases from the original peak position of T_m(H). Conversely, T_m(LII) determined from the DSC peak increases from the original position of T_m(LII). The deviation from linear T_c dependence of T_m(H) and T_m(LII) can be explained by the reason of the overlapping of these two peaks. According to this consideration, a dashed line T_m(H) is drawn in the figure.

Region III ($T_d \leq T_c$): The melting behavior is simple. Peak LIII shown in Fig. 1 corresponds to the melting of the crystals which were formed in the isothermal crystallization process. T_m(LIII) and ΔQ increase almost linearly with T_c as shown in Figs. 2 and 3. This result indicates that the crystal size and crystallinity of the ICS increase almost linearly with T_c. That is, the thermal stability of the ICS effectively increases by the isothermal crystallization. On the other hand, as will be shown in Sections 3.2 and 3.3, T_m(LIII) and ΔQ also increase with crystallization time of the ICS by the reason of the slow crystallization. That is, T_c dependence of T_m(LIII) and ΔQ shown in Figs. 2 and 3 changes with the crystallization time. However, T_m(LIII) did not largely change by the change of t_c than by the change of T_c in the present experimental conditions. The values of T_m(LIII) and ΔQ for the ICS(135 °C: 2 h), ICS (140 °C: 3 h), ICS (145 °C: 6 h), and ICS (150 °C: 12 h) are selected and plotted in Figs. 2 and 3. The effect of the crystallization time, including the reason for the selection of these data, will be discussed in the subsequent sections.

As shown in a CR–HR map in Ref. [17], the double melting behavior appears under a limited experimental condition. Accordingly, the detailed analysis on the double melting behavior has been scarcely reported. In addition, the interpretation of the experimental result on the melting process has not been taken account for the discrete change in the crystallization behavior until now. The account of the discrete changes at T_b and T_d for solving complex melting behavior suggested in this article is a fundamental difference from the others.

Recently, Di Lorenzo reported the double melting behavior of the ICS and T_c dependence of T_m and the crystallinity [19,20], which resemble to those obtained in this study. However, there are small differences in the values of T_m(H), T_m(L), and crystallinity. The discrete changes of T_m around T_b and dT_m/dT_c around T_d cannot be observed in the T_c dependence of T_m. The origin of the small differences can be interpreted by the difference of experimental conditions, HR and the starting temperature of DSC scan and temperature program of the isothermal crystallization. These small differences in the values of T_m(H), T_m(L), and crystallinity have large differences in the physical meaning on the melting behavior. That is, the discrete change of the melting behavior at $T_b = 113$ °C, which originates from the discrete change of the crystal structure, and the discrete change of dT_m/dT_c around T_d ($\sim$135 °C) cannot be presented from the T_c dependence of T_m by Di Lorenzo.

3.2. The effect of crystallization time on the melting behavior in Regions I and II

The isothermal crystallization at the crystallization time of 12 h was performed at various crystallization temperatures to

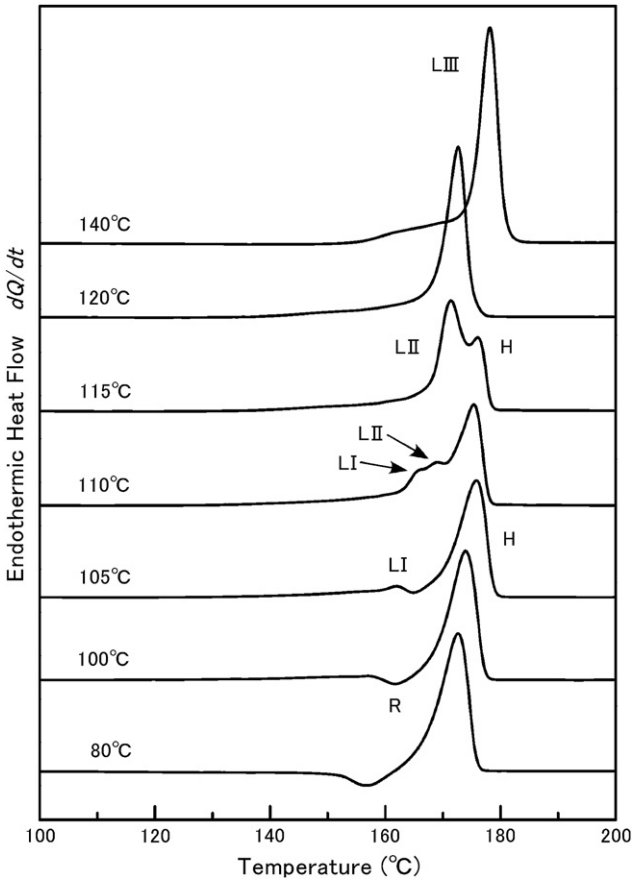

Fig. 4. DSC curves of the ICSs(12 h) obtained at the indicated T_cs. The HR of the DSC scans was 10 K min^{-1}.

study the effect of crystallization time on the melting behavior. Fig. 4 shows DSC curves of the ICSs(12 h) obtained at the indicated crystallization temperature.

Although the DSC curves shown in Fig. 4 are apparently similar to those shown in Fig. 1 at each crystallization temperature, a small difference can be observed between these DSC curves for the ICSs(110 °C, 115 °C, 120 °C). Namely, LI and LII shown in Fig. 4 are larger than those shown in Fig. 1, whereas H shown in Fig. 4 is smaller than that shown in Fig. 1. These results indicate that the thermal stability of the ICS increased by the long time isothermal crystallization, and that the reorganization in the heating process of the ICS is suppressed by the high thermal stability.

T_c dependence of the peak melting temperatures, T_m(LI), T_m(LII), T_m(LIII), and T_m(H), was obtained from the DSC curves for the ICSs(12 h) and is shown in Fig. 5. The dashed lines in the figure show the fitting curves shown in Fig. 2. T_c dependence of ΔQ was also obtained from the DSC curves for the ICSs(12 h) and is shown in Fig. 6. The dashed lines in the figure show the fitting curves shown in Fig. 3.

As shown in Fig. 5, the data points of T_m(H) almost overlap on the fitting curve. Since melting temperature corresponds to the crystal size, this result means that the size of recrystallized crystals formed in the heating process does not depend on the crystallization time of the ICS. Accordingly, it is reasonable to consider that the prolonged crystallization scarcely affects the melting of the recrystallized crystals. In contrast, T_m(L) and ΔQ depend on the crystal size and the crystallinity which were formed during the isothermal crystallization. The effect of the prolonged crystallization on T_m(L) and ΔQ and the interpretation of the crystallization at each temperature region are as follows.

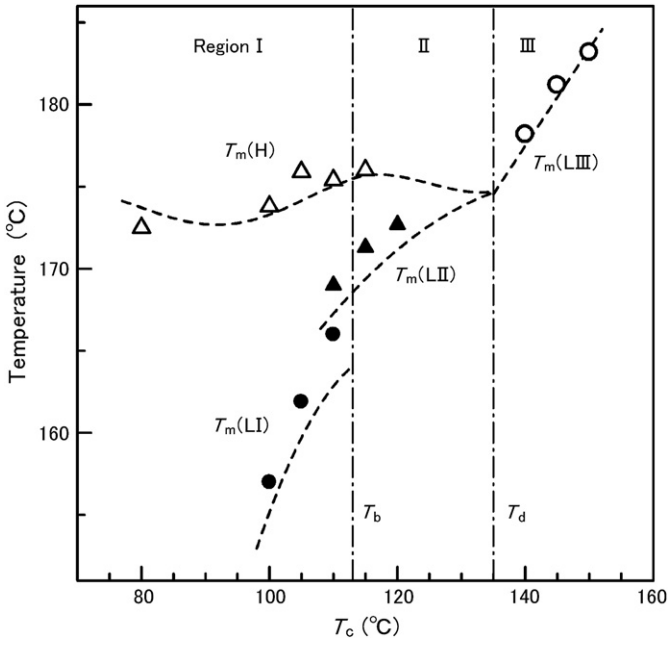

Fig. 5. T_c dependence of (●) T_m(LI) and (▲)T_m(LII), (○)T_m(LIII), and (△) T_m(H) obtained from the DSC curves of the ICSs($t_c = 12$ h). The dashed lines show the fitting curves shown in Fig. 2. The dash-dotted lines show T_b and T_d.

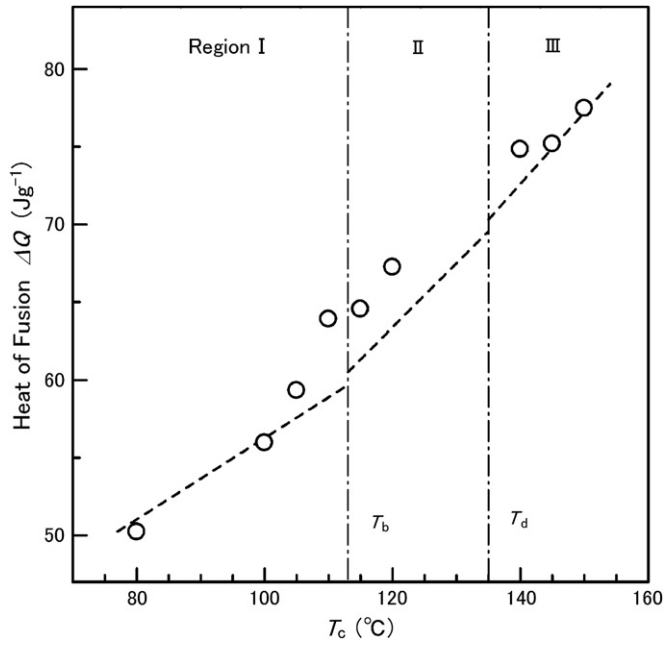

Fig. 6. T_c dependence of ΔQ calculated from the DSC curves of the ICSs(12 h). The dashed lines show the fitting curve of ΔQ values shown in Fig. 3.

Region I ($T_c \leq 100$ °C): As shown in Figs. 5 and 6, T_m(LI) and ΔQ almost overlap on the fitting curves. These results indicate that crystal size and crystallinity do not increase by the long time crystallization. That is, crystallization, lamellar thickening and perfection of the crystal scarcely proceed during the prolonged isothermal crystallization at this temperature region.

Region I ($T_c \geq 100$ °C): T_m(LI) and ΔQ increase to the respective fitting curves, and their deviation from the respective fitting curves increases with T_c. This result suggests that the crystallization, which includes reorganization of molecular chains, proceeds during prolonged isothermal crystallization, and that the rate of this crystallization increases with T_c.

Region II ($T_b \leq T_c \leq T_d$): T_m(LII) and ΔQ increase to the respective fitting curves, and the increase does not depend on T_c. This result suggests that the crystallization proceeds during prolonged isothermal crystallization, and that the increase of the rate of this crystallization does not depend on T_c.

Region III ($T_d \leq T_c$): A rate of the crystallization decreases with T_c as reported in the previous article [24]. The ICS(135 °C: 2 h), ICS(140 °C: 3 h), ICS(145 °C: 6 h), and ICS(150 °C: 12 h) were used for the DSC measurement, and DSC curves of these samples were obtained as shown in Fig. 1. Small increases of T_m(LIII) and ΔQ to the respective fitting curves in this temperature region are attributed to the effect of the prolonged isothermal crystallization. The effect of the crystallization time on the melting behavior in this temperature region is studied in detail in the Section 3.3.

3.3. The effect of crystallization time on the melting behavior in Region III

The effect of crystallization time in Region III was studied at 145 °C. Fig. 7 shows DSC curves of the ICSs(145 °C) obtained at the indicated crystallization times. As shown in the figure, an endothermic peak, an exothermic peak, and a small bump appear around 180 °C, at 114 °C, and at about 60 °C, respectively. In addition, a small endothermic peak appears at 170 °C for the ICS(1.5 h), and a broad endothermic peak appears around 165 °C for the ICSs(4.4–24 h).

The bump and the exothermic peak evidently appeared in the DSC curve of the ICS(1.5 h) correspond to the cold crystallization and the glass transition, respectively. The appearance of the bump and the exothermic peak is typical characteristics of an inclusion of the amorphous part in a starting sample. According to this assignment, it can be deduced that the crystallization scarcely proceeds in the crystallization time lower than 1.5 h, and the endothermic peak around 180 °C appeared in the DSC curve of the ICS(1.5 h) is the melting of the crystallites formed in the cold crystallization process. This deduction was confirmed by the measurement of heat of fusion. In contrast, the endothermic peaks appeared in the DSC curves of the ICSs(6, 12, 24 h) corresponds to the melting of the crystallites formed in the isothermal crystallization. That is, these peaks correspond to LIII.

Peak melting temperatures, T_ms, and the values of the heat of fusion, ΔQ, were obtained from the DSC curves of the ICSs. In this experiment, ΔQ values were calculated in the temperature range between 50 and 200 °C in the DSC curve: Total contribution of the heat due to the melting of the crystals in a starting sample (ICS), recrystallization and the melting of the crystals formed in the heating process (recrystallized crystals) were calculated. T_ms and ΔQ values are plotted against the crystallization time, t_c, in Fig. 8 with filled circles and open circles, respectively. T_m and ΔQ value for the crystallization time of 1.5 h were 177.2 °C and 7.6 J g^{-1} and are not plotted in this figure.

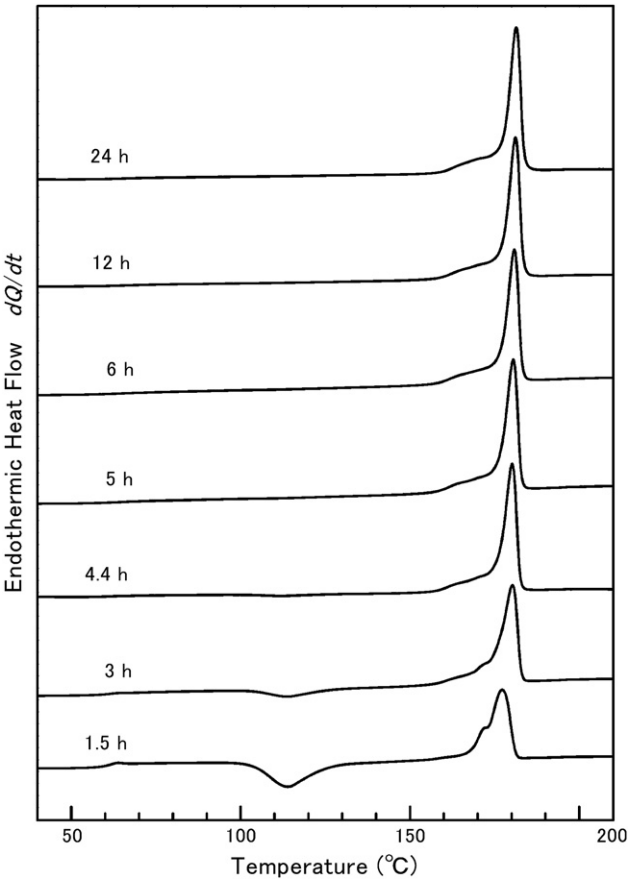

Fig. 7. DSC curves of the ICSs(145 °C) obtained at the indicated crystallization times. The HR of the DSC scans was 10 K min^{-1}.

The solid line in Fig. 8 shows the fitting curves of T_m which is fitted by the quadratic equation of log(t_c). In contrast, the fitting curve for ΔQ was obtained for two t_c regions, because the t_c dependence of ΔQ distinctly changes at 5 h. The broken lines show the fitting curves of ΔQ ($t_c \leq 5$ h) and ΔQ ($t_c \geq 5$ h) which are fitted by the linear and quadratic equations of log(t_c), respectively.

As shown in Fig. 8, ΔQ for the ICSs($t_c \leq 5$ h) logarithmically increases with t_c. That is, the crystallinity of the ICS($t_c \leq 5$ h) logarithmically increases with t_c. This result is consistent with the low growth rate of spherulites observed under polarizing microscope reported in the previous article [24]. The very low value of ΔQ for the ICS(1.5 h) suggests that induction time of the crystallization is about 1.5 h, and that the crystallization scarcely proceeds until 1.5 h at this temperature $T_c = 145$ °C. In contrast, ΔQ value for the ICSs($t_c \geq 5$ h)

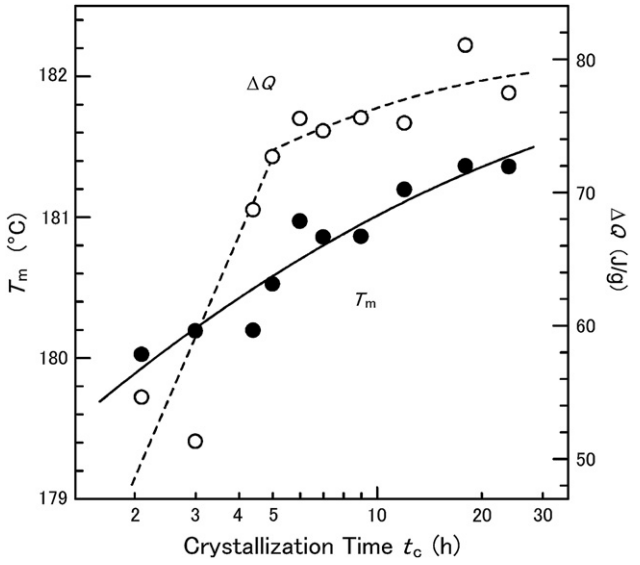

Fig. 8. Crystallization time t_c dependence of (●)T_m and (○) ΔQ obtained from the DSC curves of the ICSs(145 °C). The solid and broken lines show the fitting curves of T_m and ΔQ values, respectively.

gradually increases with log(t_c) and are in the range of 74–83 J g^{-1}. Fisher et al. reported the heat of fusion of the perfect crystal to be 92 J g^{-1} [50]. If their values are correct, the crystallinity of the ICSs($t_c \geq 6$ h) results in 80–90% by the isothermal crystallization.

As shown in Fig. 7, peak LIII for the ICSs($t_c \geq 5$ h) is sharp in comparison with that for the ICSs($t_c \leq 3$ h). On the other hand, T_m(LIII)s for the ICS(5 h) and the ICS(24 h) are 180.5 and 181.4 °C, respectively. That is, the increase of T_m(LIII) is about 0.9 K by the prolonged isothermal crystallization of 19 h. This result indicates that T_m(LIII) did not largely change by the change of t_c than by the change of T_c, and that the effect of the prolonged crystallization on the T_m(LIII) is small. The values of T_m(LIII) and ΔQ for the ICS(135 °C: 2 h), ICS(140 °C: 3 h), ICS(145 °C: 6 h), and ICS(150 °C: 12 h), whose crystallization times are the starting times of the prolonged isothermal crystallization at every crystallization temperature, are plotted in Figs. 2 and 3.

Melting temperature T_m of lamellar thickness l is given in the Thomson–Gibbs equation [52].

$$T_m = T_m^\circ\left(1 - \frac{2\sigma_e}{l\Delta h}\right) \quad (1)$$

where T_m° is the melting temperature of the infinitely large crystal (equilibrium melting temperature), σ_e the top- and bottom-specific surface free energy, l the lamellar thickness, Δh the bulk heat of fusion. The increase of the melting temperature, ΔT_m, by the increase of the lamellar thickness, Δl, is derived from Eq. (1).

$$\Delta T_m = \frac{2T_m^\circ\sigma_e}{l^2\Delta h}\Delta l \propto \frac{1}{l^2}\Delta l \quad (2)$$

As shown in Eq. (2), the increase of the lamellar thickness, Δl, is proportional to the increase of the melting temperature, ΔT_m. Besides, melting temperature of thick lamellae does not increase so much with the increase of the lamellar thickness by the factor of $1/l^2$. The reason for the small effect of the prolonged crystallization on the T_m(LIII) can be explained by the formation of the thick lamellae in the ICS(Region III).

When a sample contains small crystallites with wide size distribution, the Eqs. (1) and (2) indicate that the DSC melting peak of the sample is broad. In contrast, the DSC melting peak of a sample which contains large crystallites gives a sharp DSC melting peak, even if the crystallites have wide size distribution. From these considerations, it can be interpreted that the sharp melting peak of LIII is due to an increase of crystallite size and/or perfection by isothermal crystallization.

Fig. 9 shows X-ray diffraction patterns for the ICSs(150 °C) in the diffraction angle between 11 and 34°. Crystallization times of the ICSs are indicated in the figure. Since scattering X-ray from the amorphous part overlapped on the diffracted X-ray from the crystalline part, the X-ray diffraction patterns were obtained after the subtraction of an X-ray scattering pattern of the molten state of PLLA. The ICSs of 4.0 mm in diameter and 1.0 mm in thickness were used for the X-ray measurements, so that crystallinity of each ICS can be compared with another one by the comparison of the diffraction intensity. The diffraction pattern shows many diffraction peaks and agrees well with the orthorhombic crystal structure, which has been assigned as a HTC (α-form) [13,14,16] as reported in the previous article [24].

The ICSs(145 °C) presumably show similar t_c dependence of the X-ray diffraction pattern of the ICS(150 °C), because the difference of T_c is small (5 K). The diffraction pattern for the ICS(1.5 h) shows broad amorphous peak in the diffraction angle between 11 and 25°, and diffraction intensity of the ICS(1.5 h) is small in comparison with other diffraction patterns. This result indicates the low crystallinity of the ICS(150 °C: 1.5 h) and is consistent with the small ΔQ values for the ICS(145 °C: 1.5 h) determined from DSC and the low growth rate of spherulites observed under polarizing microscope [24].

As can be seen in Fig. 9, the diffraction intensity increases with t_c. The increasing rate of the diffraction intensity is abrupt up to 6 h and is gradual above that time. As the diffraction intensity is proportional to the crystallinity, this t_c dependence of the diffraction intensity shown in Fig. 9 supports the t_c dependence of the ΔQ values for the ICS(145 °C) determined from DSC shown in Fig. 8.

3.4. Melting temperature

T_m(H, LI, LII, LIII) changes by the crystallization condition of the ICS as mentioned in the preceding sections, and T_m also changes by the heating condition of the DSC scan, which will be shown in an article of this series. The change of each T_m by these conditions is as follows. First, T_m(H) does not largely change, because T_m(H) is the melting temperature of the recrystallized crystals. Second, T_m(LI) and T_m(LII) largely changes, because of the low thermal stability of the ICS formed in Regions I and II. Third, T_m(LIII) for the ICS

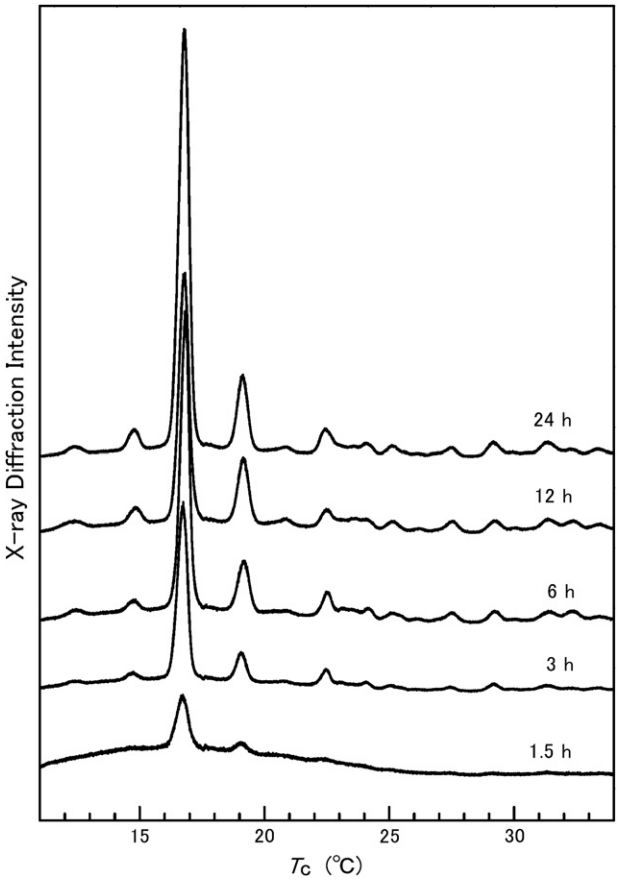

Fig. 9. X-ray diffraction patterns of the ICSs(150 °C) obtained at the indicated crystallization times.

obtained under an enough crystallization time scarcely changes by the change of the heating condition because of the high thermal stability of the ICS. In addition, it can be deduced from the t_c dependence of T_m shown in Fig. 8 that T_m(LIII) does not approach to the limiting value by the isothermal crystallization of several dozen hours. Although T_c dependence of T_m is shown in Fig. 2, it should be noted that this dependence changes by the crystallization and heating conditions, especially in Regions I and II.

The equilibrium melting temperature (T_m°) has been frequently obtained from a relationship between T_m and T_c by the Hoffman–Weeks plot method [53]. As mentioned in the previous paragraph, T_m° cannot be determined using the values of T_m(LI) and T_m(LII) of PLLA. Even if T_m(LIII) is used for the determination of T_m°, it seems that the reliability of T_m° value is not high because of the change of T_m(LIII) by t_c.

4. Conclusions

Melting behavior of PLLA was studied with DSC: DSC curves of the ICSs were obtained, and the T_c dependence of T_m and that of ΔQ were presented. Following points on the melting behavior are elucidated.

1. The melting behavior of the ICS discretely changes at T_b (=113 °C), in accordance with the discrete change of the crystallization behavior. In addition, the melting behavior changes at T_d (~135 °C) by the change of the melt-recrystallization process. That is, the melting behavior is characterized by the three temperature regions: Regions I ($T_c \leq T_b$), II ($T_b \leq T_c \leq T_d$), and III ($T_d \leq T_c$).
2. Peaks LI, H, and R appear in the DSC curve in Region I. Double melting peaks, LII and H, appear in Region II, whereas single melting peak, LIII, appears in Region III. The appearance and disappearance of the endothermic and exothermic peaks largely depend on the melt-recrystallization in the heating process. That is, they largely depend on the thermal stability of the ICS and heating conditions.
3. T_m(H) is almost constant in Regions I and II, whereas T_m(L) increases with increasing T_c. It is suggested from this fact that the crystal size of the recrystallized crystal does not largely change in the heating process. In contrast, T_c dependence of T_m(L) discretely changes at T_b: T_m(LI) discontinuously increases to T_m(LII) by 4.5 K at T_b. This discrete change in T_m(L) is in accord with the discrete change of the crystallization behavior at T_b. On the other hand, T_m(L) almost continuously changes to T_m(LIII) with T_c.
4. ΔQ almost monotonously increases with T_c, although there are small discontinuous changes of the melting behavior at T_b and T_d. The crystallinity estimated from the heat of fusion of the ICSs changes from about 55 to 83%.
5. The prolonged crystallization scarcely affects the melting of the recrystallized crystals in Region I ($T_c \leq 100$ °C). On the other hand, T_m(L) and ΔQ increase by the prolonged crystallization in Regions I ($T_c \geq 100$ °C), II, and III.
6. The effect of the prolonged crystallization on the T_m(LIII) is small. This result can be explained by the formation of the thick lamellae in the ICS(Region III). ΔQ for the ICSs(145 °C: $t_c \leq 5$ h) increases with log(t_c), whereas ΔQ values for the ICSs(145 °C: $t_c \geq 5$ h) gradually increase with log(t_c). This t_c dependence of the ΔQ values for the ICS(145 °C) determined from DSC is supported by the X-ray analysis.

Acknowledgements

The authors would like to thank Professor Chitoshi Nakafuku (Kochi University, retired) for helpful suggestions and Mr. Takao Okada (Medical Material Division, Taki Chemical Co., Ltd.) for providing us PLLA resin. We are also indebted to Dr. Shinsuke Tsubakihara (Fukuoka University) for X-ray analysis.

References

[1] Smith R, editor. Biodegradable polymers for industrial applications. Cambridge, England: Woodhead Publishing Ltd; 2005.
[2] Mallapragada S, Narasimhan B, editors. Handbook of biodegradable polymeric materials and their applications. California, USA: American Scientific Publishers; 2006.
[3] Tsuji H. Polyesters III: applications and commercial products. In: Doi Y, Steinbuchel A, editors. Biopolymers, vol. 4. Weinheim, Germany: Wiley-VCH; 2002 [chapter 5].

[4] Eling B, Gogolewski S, Pennings AJ. Polymer 1982;23:1587.
[5] Jamshidi K, Hyon SH, Ikada Y. Polymer 1988;29:2229.
[6] Celli A, Scandola M. Polymer 1992;33:2699.
[7] Nakafuku C, Sakoda M. Polym J 1993;25:909.
[8] Nakafuku C. Polym J 1994;26:680.
[9] Fambri L, Pegoretti A, Incardona SD, Migliaresi C. Polymer 1997;38:79.
[10] Iannace S, Nicolais L. J Appl Polym Sci 1997;64:911.
[11] Sarasua JR, Prud'homme RE, Wisniewski M, Borgne AL, Spassky N. Macromolecules 1998;31:3895.
[12] Mezghani K, Spruiell JE. J Polym Sci Polym Phys 1998;36:1005.
[13] Miyata T, Masuko T. Polymer 1998;39:5515.
[14] Okuzaki H, Kubota I, Kunugi T. J Polym Sci Polym Phys 1999;37:991.
[15] Lee JK, Lee KH, Jin BS. Eur Polym J 2001;37:907.
[16] Fujita M, Doi Y. Biomacromolecules 2003;4:1301.
[17] Yasuniwa M, Tsubakihara S, Sugimoto Y, Nakafuku C. J Polym Sci Polym Phys 2004;42:25.
[18] Yasuniwa M, Tsubakihara S, Sakamoto K, Takahashi K. The 55th symposium on macromolecules. Toyama: The Society of Polymer Science, Japan; 2006. p. 3507.
[19] Di Lorenzo ML. J Appl Polym Sci 2006;100:3145.
[20] Di Lorenzo ML. Macromol Symp 2006;234:176.
[21] Ling XY, Spruiell JE. J Polym Sci Polym Phys 2006;44:3200.
[22] Ling XY, Spruiell JE. J Polym Sci Polym Phys 2006;44:3378.
[23] Shieh YT, Liu GL. J Polym Sci Polym Phys 2007;45:466.
[24] Yasuniwa M, Tsubakihara S, Ono Y, Dan Y, Takahashi K. Polymer 2006; 47:7554.
[25] Holdsworth PJ, Turner AJ. Polymer 1971;12:195.
[26] Tan S, Su A, Li W, Zhou E. J Polym Sci Polym Phys Ed 2000;38: 53.
[27] Minakov AA, Mordvintsev DA, Schick C. Polymer 2004;45:3755.
[28] Hobbs SY, Pratt CF. Polymer 1975;16:462.
[29] Yasuniwa M, Tsubakihara S, Ohoshita K, Tokudome S. J Polym Sci Polym Phys Ed 2001;39:2005.
[30] Righetti MC, Lorenzo MLD, Angiuli M, Tombari E. Macromolecules 2004;37:9027.
[31] Ju MY, Chang FC. Polymer 2001;42:5037.
[32] Yasuniwa M, Tsubakihara S, Fujioka T. Thermochim Acta 2003;396:75.
[33] Yasuniwa M, Tsubakihara S, Fujioka T, Dan Y. Polymer 2005;46:8306.
[34] Cheng SZD, Cao ZQ, Wunderlich B. Macromolecules 1987;20:2802.
[35] Verma R, Marand H, Hisao B. Macromolecules 1996;29:7767.
[36] Wei CL, Chen M, Yu FE. Polymer 2003;44:8185.
[37] Yoo ES, Im SS. J Poly Sci Part B Polym Phys 1999;37:1357.
[38] Yasuniwa M, Satou T. J Polym Sci Polym Phys Ed 2002;40:2411.
[39] Yasuniwa M, Tsubakihara S, Satou T, Iura K. J Polym Sci Polym Phys Ed 2005;43:2039.
[40] Berry LG, editor. Inorganic volume PD1S-10iRB. Powder diffraction file. Philadelphia: Joint Committee on Powder Diffraction Standards; 1967. Sets 6e10 [revised].
[41] Vasanthakumari R, Pennings AJ. Polymer 1983;24:175.
[42] Tsuji H, Ikada Y. Polymer 1995;36:2709.
[43] Puiggali J, Ikada Y, Tsuji H, Lotz B. Polymer 2000;41:8921.
[44] De Santis P, Kovacs A. Biopolymers 1968;6:299.
[45] Hoogsten W, Postema AR, Pennings AJ, Brinke G, Zugenmaier P. Macromolecules 1990;23:634.
[46] Kobayashi J, Asahi T, Ichiki M, Okikawa A, Suzuki H, Watanabe T, et al. J Appl Phys 1995;77:2957.
[47] Zhang J, Tashiro K, Domb AJ, Tsuji H. Macromol Symp 2006;242:274.
[48] Zhang J, Duan Y, Sato H, Tsuji H, Noda I, Yan S, et al. Macromolecules 2005;38:8012.
[49] Okihara T, Okumura K, Kawaguchi A. J Macromol Sci Phys 2003;B42: 875.
[50] Fisher EW, Sterzel DW, Wegner G, Koll ZZ. Polymer 1973;251:980.
[51] Pyda M, Bopp RC, Wunderlich B. J Chem Thermodyn 2004;36:731.
[52] Wunderlich B. Macromolecular physics, crystal melting, vol. III. New York: Academic Press; 1980.
[53] Hoffman JD, Weeks JJ. J Chem Phys 1962;37:1723.